CATALYTIC ACTIVITY OF COBALT IMPREGNATED ON ORDERED MESOPOROUS SILICA MATERIALS IN N_2O DECOMPOSITION

KUBOŇOVÁ Lenka[1], FRIDRICHOVÁ Dagmar[1,2], PEIKERTOVÁ Pavlína[1,3], MAMULOVÁ KUTLÁKOVÁ Kateřina[3], KOZUBOVÁ Světlana[3], JIRÁTOVÁ Květuše[4], OBALOVÁ Lucie[1,5], COOL Pegie[6]

[1]Institute of Environmental Technology, [2]Energy Units for Utilization of non Traditional Energy Sources, [3]Nanotechnology Centre, [5]Faculty of Metallurgy and Materials Engineering, VSB - Technical University Ostrava, Ostrava, Czech Republic, EU
[4]Institute of Chemical Process Fundamentals of the ASCR, v.v.i., Prague, Czech Republic, EU
[6]University of Antwerp, Laboratory of Adsorption and Catalysis, Department of Chemistry, Wilrijk, Belgium, EU

Abstract

Three different ordered mesoporous silica materials, such as MCM-41, Al containing MCM-41 (mass ratio Si/Al = 10) and SBA-15, were prepared. In a next step, cobalt (5-8 wt%) as an active metal for redox reactions, was introduced by the impregnation. The prepared catalysts were characterized by AAS, EDX, N_2 physisorption, XRD, DR UV-Vis spectroscopy, Raman spectroscopy, TPR-H_2 and their catalytic properties were evaluated for N_2O decomposition and reduction. The catalysts showed poor activity in N_2O decomposition while the use of reducing agent (carbon monoxide) was beneficial for their catalytic activities. The lowest catalytic activity showed Co/Al-MCM indicating that the aggregated Co_xO_y species present in this catalyst were inactive and not beneficial for the catalytic activity.

Keywords: Mesoporous ordered silica; Aluminum; Cobalt; Impregnation; N_2O decomposition

1. INTRODUCTION

The exceptional activity of noble metals (such as Au, Rh or Ru) for the catalytic reactions such as N_2O decomposition [1, 2, 3] has been studied. However, due to the excessive cost of noble metals, the interest is paid to the use of transition metal oxide catalysts [4]. The range of papers dealing with the catalytic performance of mesoporous silica materials modified with cobalt has been published [5, 6, 7, 8, 9, 10].

The metal site isolation can be achieved by simple deposition of the metal precursor using wet impregnation. However, the impregnation method often results in catalysts with broader distribution of metal species and lower degree of dispersion or bulk oxide. Metal acetylacetonate (acac) complex such as $VO(acac)_2$ was used for the wet impregnation of vanadium on hexagonal mesoporous silica (HMS) as reported by Bulanek and co-authors [11]. The similar approach was applied in our study. As reported in the papers [12, 13], the adsorption of $Co(acac)_2$ complexes leaded to the precipitation of cobalt oxides on alumina surface. On the other hand, the stability of $Co(acac)_2$ was beneficial to form a high loading of cobalt on silica surface.

Aluminum is known as an element generating acid sites by substitution of Si by Al in the silica structure. Aluminum can enhance the dispersion, localization and stability of metal nanoparticles (such as Fe, Ru, Rh or Au) on silica surface such as SBA-15 or SiO_2 extracted from the natural clay [3, 14].

To our knowledge, the catalysts prepared by impregnation of $Co(acac)_2$ on ordered mesoporous silica materials (MCM-41, MCM-41 with incorporated aluminum and SBA-15) and tested in N_2O catalytic decomposition and reduction by using CO as the reducing agent have not been reported yet. The aim of the paper is to find the relation among physicochemical properties of cobalt deposited on different supports and the performance of these materials in the above mentioned catalytic reactions. The main interest is focused on the differences in (i) textural and structural properties of catalysts supports, (ii) crystalline phase, (iii) coordination and oxidation state of cobalt cations and (iv) reducibility of catalysts.

2. MATERIALS AND METHODS

Synthesis of mesoporous silica supports

MCM-41 material was prepared by a direct interaction between an ionic, positively charged surfactant and a negatively charged silica source in a basic environment. The synthesis of MCM-41 was performed according to [15] by using cetyltrimethylammonium bromide (C_{16}TMABr), ammonia (30 wt% solution of NH_3 in H_2O), tetraethyl orthosilicate (98 % TEOS) and water.

Synthesis of Al-MCM-41 was done according to [16]. Sodium hydroxide (NaOH), cetyltrimethylammonium bromide (CTABr, $C_{16}H_{33}(CH_3)_3NBr$), tetraethylorthosilicate (TEOS), aluminum sulphate ($Al_2(SO)_4 \cdot 18H_2O$), and deionized water were used.

SBA-15 material was prepared by use of block copolymeric surfactant that interacts with the positively charged silica source in acid medium. SBA-15 was synthesized as described in [17] in acidic conditions using polyethyleneoxide-polypropyleneoxide-polyethyleneoxide copolymer ($EO_{20}PO_{70}EO_{20}$), hydrochloric acid (37 % HCl), tetraethyl orthosilicate (98 % TEOS) and water.

Preparation of catalysts

The calcined silica support was dried in an oven at 200 °C in the air atmosphere. The appropriate amount of $Co(acac)_2$ was dissolved in ethanol. Afterwards, the calculated amount of support was added to the solution which was stirred at 80 °C till ethanol slowly evaporated. Finally, the formed suspension was dried in the oven at 120 °C and calcined at 550 °C with a heating rate of 1 °C.min^{-1} in the period of 12 h.

The prepared catalysts are designed as: (i) Co/MCM, (ii) Co/Al-MCM, and (iii) Co/SBA.

Characterization techniques

The metal loadings were determined by an electron dispersive X-ray (EDX) analyzer XL30 Phillips and by an atomic absorption spectrometer (AAS) Spectr AA880 (Varian). For AAS analysis, the catalysts were dried, dissolved in 3 ml HCl and heated up.

Textural properties of the samples were determined by nitrogen sorption measurements at -196 °C using a QuadraSorb SI MP Station. Prior to the measurements, the samples were degassed under vacuum at 200 °C for 16 h. The mesopore diameter was determined from the maximum of pore size distribution curve of BJH method. The microporosity was evaluated by t-plot method using de Boer for oxidic silicas.

The XRD patterns in 2θ range from 10 to 80° were recorded under CoKα irradiation (λ = 1.789 Å) using the Bruker D8 Advance diffractometer (Bruker AXS) equipped with a fast position sensitive detector VÅNTEC 1. Measurements were carried out in the reflection mode, powder samples were pressed in a rotational holder, goniometer with the Bragg-Brentano geometry in 2 θ range from 5 to 60°. Phase composition was evaluated using database PDF-2 Release 2011 (International Centre for Diffraction Data).

Diffuse reflectance UV-Vis spectra of the powder samples were recorded in the range 190 - 900 nm (11111 - 50000 cm^{-1}) at room temperature on the Cintra 303 equipped with a diffuse reflectance attachment.

Raman spectra were measured by Smart Raman Microscopy System XploRA™ (HORIBA Jobin Yvon, France). Raman spectra were acquired with 532 nm excitation laser source, and 2400 groove/mm grating in the range 150 - 1100 cm^{-1}. Raman spectra were acquired at each of at least 5 points.

Temperature programmed reduction by hydrogen (TPR-H_2) was carried out on AutoChemII 2920 on the powder samples of the grain 0.160-0.315 mm. The TPR runs were performed in the flow of 10 vol% H_2/Ar (50 ml.min^{-1}) with the heating rate 20 °C.min^{-1}in the temperature range 25-1000 °C. The hydrogen consumption was monitored by thermal conductivity detector (TCD).

The cobalt standards CoO (Alfa Aesar, CAS: 1307-96-6, purity 95 %), Co_3O_4 (Alfa Aesar, CAS: 1308-06-1, purity 99.7 %) and $CoAl_2O_4$ (Alfa Aesar, CAS: 12672-27-4, Co 39-41 %) were applied.

Catalytic tests

The catalytic tests were performed in an integral fixed bed stainless steel reactor of 5 mm internal diameter in the temperature range from 390-450 °C under atmospheric pressure. The catalyst bed contained 0.1 g of catalyst with a particle size of 0.160-0.315 mm. The weight hourly space velocity (WHSV) of 60 000 l h^{-1} kg^{-1} (GHSV = 15648 h^{-1}) was applied. The feed introduced to the reactor contained (i) 0.1 mol% N_2O in nitrogen and (ii) 0.1 mol% N_2O and 0.1 mol% CO in nitrogen. A gas chromatograph equipped with a thermal conductivity detector (TCD) (Agilent Technologies 7890A) and the chromatographic column ShinCarbon Micropacked (dimension: 2 m x 0.53 mm, oven program: 100 °C for 2 min then 40 °C/min to 250 °C for 1 min) was used for N_2O analysis.

3. RESULTS AND DISCUSSIONCharacterization of catalysts

Theoretical and experimental Si/Al ratio, initial loadings of $Co(acac)_2$, theoretical concentration of Co and final concentrations of Co and Al determined by EDX and AAS analyses are displayed in **Table 1**. AAS measured the bulk concentration of cobalt and is more precise than EPMA measuring only surface concentration of cobalt. The concentration of cobalt determined by AAS is considered for further comparison of catalysts.

Table 1 Initial concentrations of $Co(acac)_2$ and final concentrations of Al and Co in the catalysts

Sample	Final Al conc.[a]	Si/Al		Initial Co $(acac)_2$ conc.	Theor. Co conc.	Final Co conc.
	wt %	-		$mmol.g^{-1}$	wt %	wt %
Co/MCM	-		-	1.7	10	6.7[b], 5.2[c]
Co/Al-MCM	4.1	17[a]	9.7[b]	1.7	10	6.9[b], 7.4[c]
Co/SBA	-		-	1.7	10	4.7[b], 7.7[c]

[a] Theoretical Si/Al ratio. Si/Al are mass ratios.

[b] EDX analysis, [c] AAS analysis.

The evaluated textural properties of prepared catalysts are summarized in **Table 2**. The Co/MCM has the highest surface area whereas Co/SBA has the highest mesopore diameter with the presence of micropores in the mesopore structure.

Table 2 Results of textural properties of Co-impregnated catalysts

Sample	S_{BET}	S_{micro}	V_{total}, p/p_0 = 0.99-1.0	V_{micro}	d_{pore}
	$m^2.g^{-1}$	$m^2.g^{-1}$	$cm^3.g^{-1}$	$cm^3.g^{-1}$	nm
Co/MCM	1256	-	1.03	-	2.8
Co/Al-MCM	605	-	0.46	-	2.7
Co/SBA	569	172	0.76	0.08	5.7

The Co spinel phase was surely detected in Co/Al-MCM catalyst. XRD patterns of other catalysts are noisy for the determination of Co spinel phase. Due to the similar reflection angles and intensities in XRD, it is not possible to distinguish between Co_3O_4 (PDF number 65-3103), $CoAl_2O_4$ (PDF number 03-0896) and Co_2AlO_4 (PDF number 02-1410). As depicted in **Fig. 1**, the peak of amorphous SiO_2 at the maximum 2Θ = 27 ° is the most apparent in Co/SBA catalyst.

The DR UV-Vis spectra are used for the characterization of the nature and the coordination of cobalt oxide species. Triplet absorption bands at around 15550, 17094, 19120 cm^{-1} are assigned to $^4A_2(F) \rightarrow {}^4T_1(P)$ transition of Co(II) species in tetrahedral coordination geometry, see **Fig. 2** [18, 19, 20].

The absorption band at 13642 and 23310 cm^{-1} are attributed to non-specified oxide Co_xO_y, as it is obvious in **Fig. 2** [20, 21]. These bands are evident in Co/Al-MCM.

Raman spectroscopy is much more sensitive for the detection of small crystalline clusters than XRD analysis [22]. **Fig. 3** shows Raman spectra of Co-impregnated catalysts where five bands at 194, 479, 520, 612, and 682 cm^{-1} are clearly visible. According to the literature [23], these bands correspond to symmetric vibrational modes F_{2g}, E_g, F_{2g}, F_{2g}, and A_{1g} and predict the formation of microcrystallites of Co_3O_4. The measured Raman spectra of cobalt standards Co_3O_4, CoO and $CoAl_2O_4$ are shown in **Fig. 4**. By comparison of the spectra, the determination of Co_3O_4 and/or CoO is difficult due to their similar spectra as well as the position of the bands in Co-impregnated catalysts could be affected by the presence of supports. The phase $CoAl_2O_4$ is not present in the catalysts by comparison of **Figs. 3, 4** as well as Co_2AlO_4 and $NaCo_2O_4$ are not present, according to the literature [24].

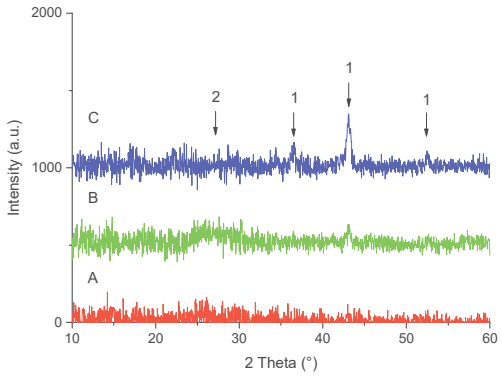

Fig. 1 XRD patterns of catalysts A) Co/MCM, B) Co/SBA and C) Co/Al-MCM. The phases are: 1 - cobalt spinel, 2 - amorphous SiO_2

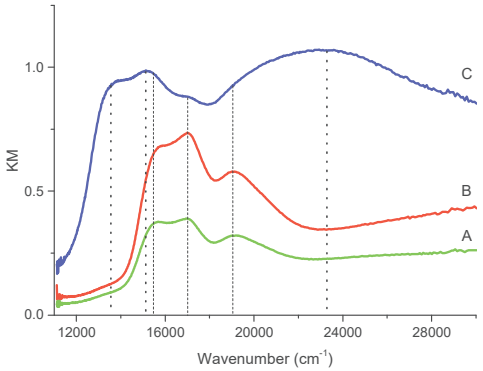

Fig. 2 DR UV-vis spectra of catalysts A) Co/SBA, B) Co/MCM and C) Co/Al-MCM

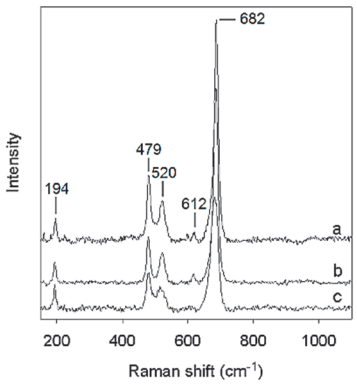

Fig. 3 Raman spectra of Co/SBA (a), Co/Al-MCM (b), Co/MCM (c) catalysts

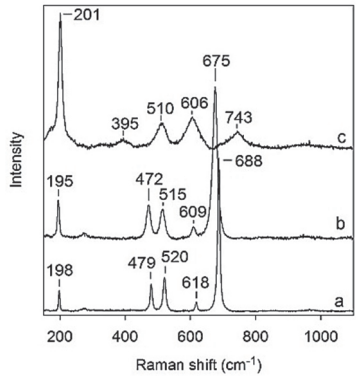

Fig. 4 Raman spectra of the standards Co_3O_4 (a), CoO (b), and $CoAl_2O_4$ (c)

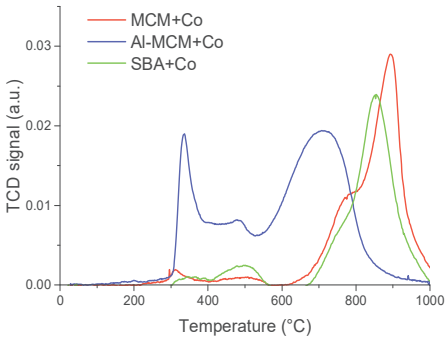

Fig. 5 TPR-H_2 profiles of Co-impregnated catalysts

The results from TPR-H_2 of Co-impregnated catalysts and cobalt standards are summarized in **Table 3**. The TPR profiles are depicted in **Fig. 5**. The low-temperature reduction peaks (25-500 °C) correspond to the reduction of $Co^{III} \rightarrow Co^{II}$ and/or $Co^{II} \rightarrow Co^0$ in cobalt oxides [25]. The highest amount of easily reducible cobalt species was present in Co/Al-MCM indicating that the sintering of Co particles into aggregates was favored in this catalyst. The high-temperature reduction peaks (530-1000 °C) are assigned to Co^{2+} ions interacting strongly with the support and to the reduction of surface Co silicate [10, 26]. The broad second reduction peak with T_{max} 709 °C in the catalyst Co/Al-MCM indicates less uniform cobalt ion distribution in the silica framework [9]. Compared to that, Co/MCM and Co/SBA catalysts showed significant shift of T_{max} to higher temperature indicating higher reduction stability of these catalysts.

Table 3 The results from TPR-H_2 experiments and catalytic tests

Sample	T_{max}	H_2 consumed	H_2 consumed	N_2O decomposition	N_2O reduction	TOF
	25- 1000°C	25- 500°C	25- 1000°C	X_{N2O}	X_{N2O}	
	°C	mmol.g_{sample}^{-1}	mmol.g_{sample}^{-1}	%	%	h^{-1}
Co/MCM	310, 894	0.12	1.01	2	17	254
Co/Al-MCM	335, 709	0.29	1.47	4	13	125
Co/SBA	495, 855	0.21	0.97	5	37	359
CoO	464	16.16	-	-	-	-
Co_3O_4	400	19.50	-	-	-	-
$CoAl_2O_4$	397, 977	2.63	4.59	-	-	-

Catalytic activity in N_2O decomposition and reduction

The Co-impregnated catalysts were tested in N_2O decomposition. The N_2O conversion (X_{N2O}) at 450 °C was in the order: Co/SBA > Co/Al-MCM > Co/MCM which indicates no catalytic activity in N_2O decomposition for all catalysts.

The rate determining step of catalytic decomposition of N_2O (Eq. 1) is supposed to be the reduction of active sites to remove adsorbed oxygen species which remain on the surface after dissociation of N_2O molecule.

$$N_2O \rightarrow N_2 + ½\ O_2 \quad (1)$$

Therefore, reducing agent (such as carbon monoxide) could facilitate desorption of oxygen species and hence the rate of N_2O decomposition (Eq. 2).

$$N_2O + CO \rightarrow N_2 + CO_2 \quad (2)$$

The reducing agent increased the activity (X_{N2O} at 450 °C) which was in the order: Co/SBA > Co/MCM > Co/Al-MCM. The catalytic activity expressed by TOF (turnover frequency) as the number of N_2O molecules reacting in unit time per active cobalt site defined by AAS [27] was at 450 °C in the order: Co/SBA > Co/MCM > Co/Al-MCM reflecting the highest activity of Co/SBA catalyst. The Co/SBA catalyst does not differ from Co/MCM from the point of view of the coordination and oxidation state of cobalt assigned to surface Co(II) species in tetrahedral coordination geometry. Therefore, the reason for higher activity can be due to different particle size of cobalt and its dispersion on silica supports. The Co/Al-MCM differs from the others indicating the presence of aggregated Co_xO_y species which showed up to be inactive and not beneficial for the catalytic N_2O decomposition and reduction even though the reducibility below 500 °C was the highest for Co/Al-MCM.

4. CONCLUSIONS

The impregnation method was applied for the deposition of cobalt on three different mesoporous silica supports: MCM-41, MCM-41 with aluminum incorporated into the silica framework (Al-MCM-41) and SBA-15.

The presence of tetrahedral Co(II) was detected for all prepared catalysts, however, the presence of aggregated crystalline Co_xO_y species was analyzed by XRD, DR UV-Vis and TPR-H_2 in Co/Al-MCM. There is no clear determination by Raman spectroscopy of CoO or Co_3O_4 crystalline phase.

The catalysts showed no activity in the reaction of N_2O decomposition whereas the use of reducing agent (carbon monoxide) increased their catalytic activities. However, N_2O conversion did not exceed 37 % at 450°C in the case of Co/SBA. The lowest catalytic activity showed Co/Al-MCM indicating that aggregated Co_xO_y species on the surface of Co/Al-MCM were inactive and not beneficial for the catalytic activity.

ACKNOWLEDGEMENTS

The presented work was financially supported by Grant Agency of the Czech Republic (project no. GA14-13750S), by Ministry of Education, Youth and Sports of the Czech Republic in the "National Feasibility Program I", project LO1208", by the project "ENET" (No. CZ.1.05/2.1.00/03.0069) and by SGS 2015/125.

REFERENCES

[1] CHMIELARZ, L. et al. SBA-15 mesoporous silica modified with metal oxides by MDD method in the role of $DeNO_x$ catalysts. Microporous and Mesoporous Materials, Vol. 127, 2010, pp. 133-141.

[2] HUSSAIN, M., FINO, D., RUSSO, N. Development of modified KIT-6 and SBA-15-sperical supported Rh catalysts for N_2O abatement: From powder to monolith supported catalysts. Chemical Engineering Journal, Vol. 238, 2014, pp. 198-205.

[3] XU, X. et al. SBA-15 based catalysts in catalytic N_2O decomposition in a model tail-gas from nitric acid plants. Applied Catalysis B: Environmental, Vol. 53, 2004, pp. 265-274.

[4] ROYER, S., DUPREZ, D. Catalytic oxidation of carbon monoxide over transition metal oxides. Chem.Cat.Chem, Vol. 3, 2001. pp. 24-65.

[5] BHOWARE, S.S., KAMBLE, K.R. Catalytic activity of cobalt containing MCM-41 and HMS in liquid phase oxidation of diphenylmethane. Catalysis Letters, Vol. 133, 2009, pp. 106-111.

[6] FARZANEH, F., JALALIAN, M., TALEBI, L. Epoxidation of alkenes with molecular oxygen catalyzed by immobilized $Co(acac)_2$ and $Co(bpy)_2Cl_2$ complexes within nanoreactors of Al-MCM-41. E-Journal of chemistry, Vol. 9, No. 4, 2012, pp. 2205-2212.

[7] PRIETO, G. et al. Cobalt supported on morphologically tailored SBA-15 mesostructures: The impact of pore length on metal dispersion and catalytic activity in the Fischer-Tropsch synthesis. Applied Catalysis A-General, Vol. 367, 2009, pp. 146-156.

[8] TANG, C. et al. An efficient strategy for highly loaded, well dispersed and thermally stable metal oxide catalysts. Catalysis Communications, Vol. 12, 2011, pp. 1075-1078.

[9] WANG, C. et al. Synthesis, characterization and catalytic performance of highly dispersed Co-SBA-15. Journal of Physical Chemistry C, Vol. 113, No. 33, 2009, pp. 14863-14871.

[10] WANG, H. et al. Sulfur doped Co/SiO_2 catalysts for chirally selective synthesis of single walled carbon nanotubes. Chemical communications, Vol. 49, 2013, pp. 2031-2033.

[11] BULÁNEK, R. et al. Effect of preparation method on nature and distribution of vanadium species in vanadium-based hexagonal mesoporous silica catalysts: Impact on catalytic behavior in propane ODH. Applied Catalysis A: General, Vol. 415-416, 2012, pp. 29-39.

[12] VOORT VAN DER, P. et al. The uses of polynuclear metal complexes to develop designed dispersions of supported metal oxides: Part I. Synthesis and characterization. Interface science, Vol. 5, 1997, pp. 169-197.

[13] VAN VEEN, J.A.R., JONKERS, G., HESSELNIK, W.H. Interaction of transition-metal acetylacetonates with γ-Al_2O_3 surfaces. Journal of the Chemical Society, Faraday Transactions, Vol. 85, No. 2, 1989, pp.389-413.

[14] ZHANG, F. et al. Clay-based SiO_2 as active support of gold nanoparticles for CO oxidation catalyst: Pivotal role of residual Al. Catalysis Communications, Vol. 35, 2013, pp. 72-75.

[15] LIU, S. et al. The influence of the alcohol concentration on the structural ordering of mesoporous silica: cosurfactant versus cosolvent. Journal of Physical Chemistry B, Vol. 107, 2003, pp. 10405-10411.

[16] POLADI, R.H.P.R. and LANDRY, C.C. Synthesis, characterization and catalytic properties of microporous/mesoporous material, MMM-1. Journal of Solid State Chemistry, Vol. 167, 2002, pp.363-369.

[17] MEYNEN, V., COOL, P. and VANSANT, E.F. Verified syntheses of mesoporous materials. Microporous and Mesoporous Materials, Vol. 125, 2009, pp. 170-223.

[18] BHOWARE, S.S., SINGH, A.P. Characterization and catalytic activity of cobalt containing MCM-41 prepared by direct hydrothermal, grafting and immobilization methods. Journal of Molecular Catalysis A: Chemical, Vol. 266, 2007, pp. 118-130.

[19] JANAS, J. et al. Effect of Co content on the catalytic activity of CoSiBEA zeolite in the selective catalytic reduction of NO with ethanol: Nature of the cobalt species. Applied Catalysis B: Environmental, Vol. 75, 2007, pp. 239-248.

[20] ZHANG, F. et al. NO SCR with propane and propene on Co-based alumina catalysts prepared by co-precipitation. Applied Catalysis B: Environmental, Vol. 73, 2007, pp. 209-219.

[21] SZEGEDI, Á., POPOVA, M., MINCHEV, C. Catalytic activity of Co/MCM-41 and Co/SBA-15 materials in toluene oxidation. Journal of Material Science, Vol. 44, 2009, pp. 6710-6716.

[22] BALTES, M. Supported tantalum oxide and supported vanadia-tantala mixed oxides. Journal of Physical Chemistry B, Vol. 105, 2001, pp. 6211-6220.

[23] NA, C. W. et al. Controlled transformation of ZnO nanobelts into CoO/Co_3O_4. CrystEngComm, Vol. 14, 2012, pp. 3737-3741.

[24] LEE, H.S. et al. High thermoelectric power in a Na_xCoO_2 thin film prepared by sputtering with rapid thermal annealing. Current Applied Physics, Vol. 15, 2015, pp. 412-416.

[25] OBALOVÁ, L. et al. Effect of potassium in calcinated Co-Mn-Al layered double hydroxide on the catalytic decomposition of N_2O. Applied Catalysis B: Environmental, Vol. 90, 2009, pp. 132-140.

[26] SIMIONATO, M., ASSAF, E.M. Preparation and Characterization of Alumina-Supported Co and Ag/Co Catalysts. Materials Research, Vol. 6, No. 4, 2003, pp. 535-539.

[27] PAC. Manual of Symbols and Terminology for Physicochemical Quantities and Units - Appendix II. Definitions, Terminology and Symbols in Colloid and Surface Chemistry. Part II: Heterogeneous Catalysis. Vol. 46, 1976, pp. 81.